Bayesian Feedback Control of a Two-Atom Spin-State in an Atom-Cavity System

Stefan Brakhane,[1,*] Wolfgang Alt,[1] Tobias Kampschulte,[1] Miguel Martinez-Dorantes,[1] René Reimann,[1] Seokchan Yoon,[1] Artur Widera,[2] and Dieter Meschede[1]

[1]Institut für Angewandte Physik der Universität Bonn, Wegelerstrasse 8, 53115 Bonn, Germany
[2]Fachbereich Physik der TU Kaiserslautern und Landesforschungszentrum OPTIMAS, Erwin-Schrödinger-Strasse, 67663 Kaiserslautern, Germany

(Received 14 June 2012; published 23 October 2012)

We experimentally demonstrate real-time feedback control of the joint spin-state of two neutral cesium atoms inside a high finesse optical cavity. The quantum states are discriminated by their different cavity transmission levels. A Bayesian update formalism is used to estimate state occupation probabilities as well as transition rates. We stabilize the balanced two-atom mixed state, which is deterministically inaccessible, via feedback control and find very good agreement with Monte Carlo simulations. On average, the feedback loop achieves near optimal conditions by steering the system to the target state marginally exceeding the time to retrieve information about its state.

DOI: 10.1103/PhysRevLett.109.173601 PACS numbers: 42.50.Pq, 42.50.Lc

Two or more quantum systems sharing a single excitation are forming joint quantum states, also called Dicke states. They are important building blocks for controlled quantum systems with applications in, e.g., quantum communication [1,2] or quantum simulation [3]. Experimental realizations are based on several different platforms including trapped ions [4], cold atoms [5], artificial atoms, and circuit cavity QED systems [6].

Schemes based on both deterministic [7] and probabilistic [8] methods have been proposed for the creation of joint quantum states in a cavity QED system. In practice, passive or dynamic measures are used to reduce the influence of external disturbances and decoherence needed to approach a unitary evolution of the many particle system. In this Letter we demonstrate that the application of active feedback schemes can significantly extend tight control [9], i.e., the fidelity of the processes creating joint two-particle quantum states, beyond purely passive deterministic or probabilistic state preparation.

A proposal by Balykin and Lethokhov [10] called a feedback method "information cooling" for motional control of atoms, emphasizing the close connection of information and control. Feedback control leading to cooling was recently realized [11,12] with atoms strongly coupled to a high-finesse optical resonator. The method is successful at the single particle level in the strong coupling limit of cavity QED: The transmission of the optical resonator allows real-time monitoring of the atomic position and motional control via modulation of a trapping potential.

Here, in contrast, we focus on feedback onto the internal atomic state: We experimentally perform projective measurements to discriminate the joint discrete two-atom quantum states $\hat{\rho}_{\alpha=0} \equiv |\downarrow\downarrow\rangle\langle\downarrow\downarrow|$, $\hat{\rho}_{\alpha=1} \equiv 1/2(|\uparrow\downarrow\rangle\langle\uparrow\downarrow| + |\downarrow\uparrow\rangle\langle\downarrow\uparrow|)$ and $\hat{\rho}_{\alpha=2} \equiv |\uparrow\uparrow\rangle\langle\uparrow\uparrow|$, where α corresponds to the number of atoms in the spin up state, and invokes actuators to drive the system towards the target state $\hat{\rho}_{\alpha=1}$. For optimal feedback loop operation the time to correct a state should not exceed the measurement time needed to detect a deviation from the target state. Thus, a rapid and efficient processing of the limited information retrieved from the system in the presence of quantum and technical noise is essential. We use an algorithm [13] based on Bayes' rule [14] for conditional probabilities. It assigns and updates time-dependent probabilities $p_\alpha(t)$ to the quantum states $\hat{\rho}_\alpha$ after every individual measurement of the number of transmitted photons $n(t)$ for a bin time Δt, using the contained information in an optimal way. We achieve a correction of our state after a time of 1.12 times the measurement time bin, thus approaching optimal feedback response efficiency.

In our experiment, the pseudospin states are implemented by the two long-lived hyperfine ground states $|F=3\rangle = |\downarrow\rangle$ and $|F=4\rangle = |\uparrow\rangle$ of cesium. We trap two laser-cooled Cs atoms inside a high finesse optical cavity using a far off-resonant standing wave dipole trap, see Fig. 1(a) [15,16]. The cavity resonance frequency is blue detuned from the $F = 4 \rightarrow F' = 5$ transition of the Cs D_2-line and is on

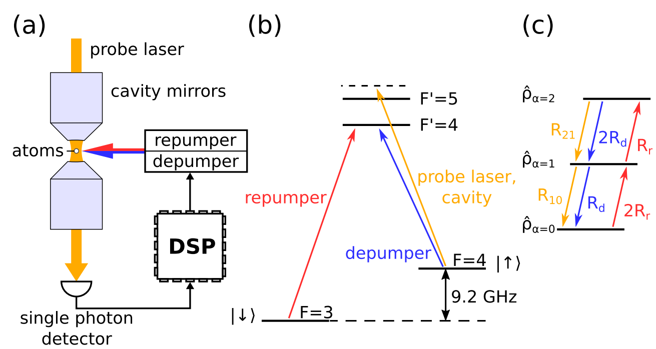

FIG. 1 (color online). (a) Schematic of experimental setup, (b) simplified level scheme of Cs, (c) two-atom states and transition rates of probe (R_{21},R_{10}), repumping (R_r) and depumping (R_d) laser.

resonance with the frequency of a weak probe laser, see Fig. 1(b).

The detuning of the cavity from the atomic resonance and the position of atoms inside the cavity mode are optimized to achieve long storage times of the atoms and maximally spaced transmission levels: The two-atom states $\hat{\rho}_{\alpha=0,1,2}$ reduce the probe laser transmission by 0%, 30%, 60% to resolve the different atomic states with the highest contrast [13]. While the driving of the atom-cavity system by the probe laser allows us to continuously obtain information about the joint atom state via the transmitted light, the probe beam itself also induces spontaneous transitions $\hat{\rho}_{\alpha=2(1)} \rightarrow \hat{\rho}_{\alpha=1(0)}$ by inelastic Raman scattering at rates R_{21} (R_{10}), see Fig. 1(c).

The cavity transmission is measured by a single photon counter [15] which is connected to a digital signal processor (DSP) controlling the intensities of both a repumping laser (rate R_r, $F = 3 \rightarrow F = 4$) and a depumping laser (rate R_d, $F = 4 \rightarrow F = 3$) in real time, see Fig. 1.

To exclude atom losses during the experiment, we determine the number of atoms via fluorescence at the beginning and the end of each experimental sequence and we measure the cavity transmission after optical pumping to $\hat{\rho}_{\alpha=2}$ at the end to exclude positioning errors leading to bad coupling.

For the estimation of the rates we choose continuous weak repumping laser intensities ($R_d = 0$, $R_r \approx R_{10}$), at which we observe abrupt state changes called quantum jumps as shown in Fig. 2(a) [13].

We estimate the state of the system by assigning occupation probabilities $\mathbf{p}(t) = (p_0(t), p_1(t), p_2(t))^T$ to the states $\hat{\rho}_\alpha$. At discrete times spaced by the bin time Δt we determine the number of transmitted photons $n(t_i)$. Application of Bayes' theorem [14] yields *a posteriori* state probabilities from *a priori* probabilities $p_\alpha^{\mathrm{pri}}(t_i)$,

$$p_\alpha^{\mathrm{post}}(t_i) = p[\alpha|n(t_i)] = \frac{p[n(t_i)|\alpha]\, p_\alpha^{\mathrm{pri}}(t_i)}{\sum_\beta p[n(t_i)|\beta]\, p_\beta^{\mathrm{pri}}(t_i)}, \quad (1)$$

based on the distribution of conditional probabilities $p[n|\alpha]$ for the same bin time. These distributions are known from photon count histograms of separately measured cavity transmissions for exactly 0, 1, 2 atoms optically pumped to strongly couple to the cavity, see right diagram in Fig. 2. With no further information available the *a posteriori* probabilities would become the *a priori* probabilities for the following measurement, $\mathbf{p}^{\mathrm{post}}(t_i) \rightarrow \mathbf{p}^{\mathrm{pri}}(t_{i+1})$. This procedure can be interpreted as repeated updating of our knowledge about the state of the system based on the measured number of photons $n(t_i)$. The initial *a priori* probabilities $\mathbf{p}^{\mathrm{pri}}(t_0) = (0, 0, 1)^T$ are assigned according to the state $\hat{\rho}_{\alpha=2}$

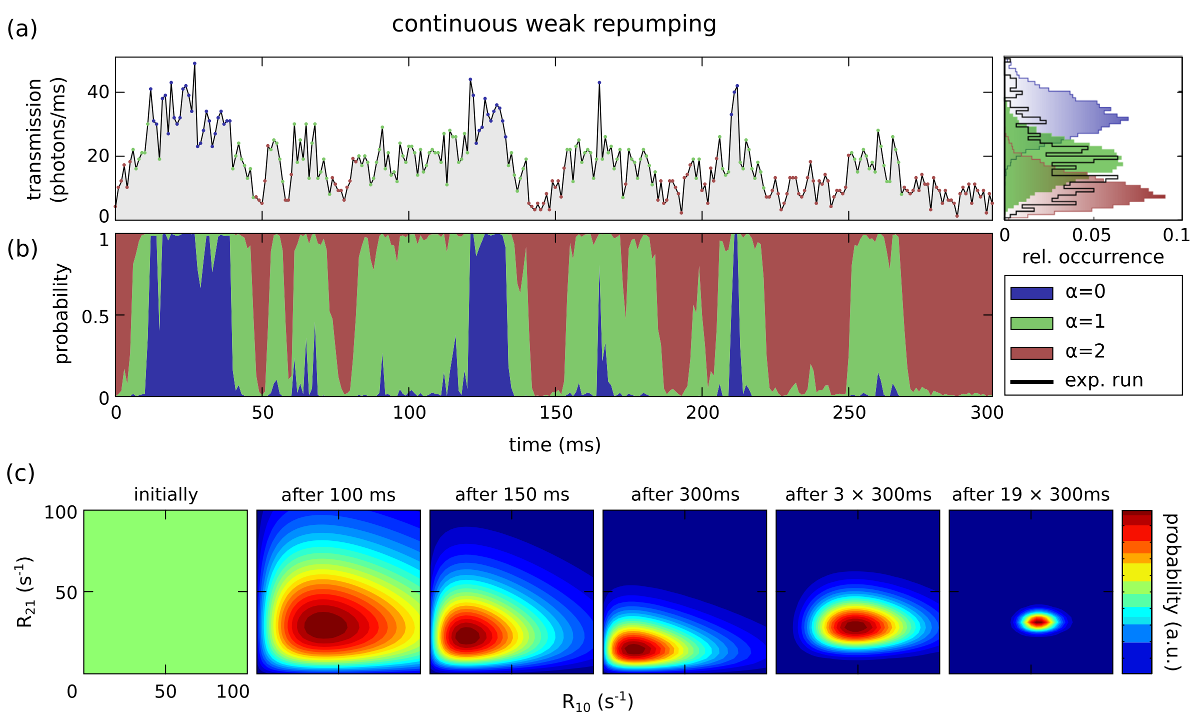

FIG. 2 (color online). (a) Detected number of transmitted photons $n(t_i)$ through the cavity for continuous weak repumping for a bin time of $\Delta t = 1$ms. Right: The corresponding photon count histogram of $n(t_i)$ (black curve) is shown in comparison to separately measured photon count histograms $p[n|\alpha]$ for $\alpha = 0, 1, 2$ coupled atoms (shaded areas). (b) Estimated probabilities $p_\alpha^{\mathrm{post}}(t_i)$, which are computed in real time according to the Bayesian update formalism based on $n(t_i)$ as shown in (a). (c) Evolution of the Bayesian probabilities of the quantum jump rates starting from a uniform *a priori* distribution over 19 successive transmission measurements of 300 ms each. (a.u., arbitrary units.)

prepared by optical pumping at the beginning of each experimental sequence.

The average evolution of our system is described by rate equations. Thus we can further improve our knowledge of the *a priori* system state at time t_{i+1} by taking into account the evolution from the previous *a posteriori* system state $\mathbf{p}^{\text{post}}(t_i)$. For weak continuous repumping [rates $\{R_j\} = \{R_{21}, R_{10}, R_r\} \ll \Delta t^{-1}$, Fig. 1(c)] the linearized solution is

$$\mathbf{p}^{\text{pri}}(t_{i+1}) = \left[\mathbb{1} + \Delta t \begin{pmatrix} -2R_r & R_{10} & 0 \\ 2R_r & -R_{10} - R_r & R_{21} \\ 0 & R_r & -R_{21} \end{pmatrix} \right] \cdot \mathbf{p}^{\text{post}}(t_i), \tag{2}$$

where $\mathbb{1}$ is the 3×3 identity matrix.

The model implemented by Eq. (2) allows us to extend Bayes' theorem to generalized probabilities $p(\alpha, \{R_j\})$ for states *and* rates, overcoming the need to determine $\{R_j\}$ by an independent measurement:

$$p^{\text{post}}[\alpha, \{R_j\} | n(t_i)] \propto p[n(t_i)|\alpha] \, p^{\text{pri}}(\alpha, \{R_j\}). \tag{3}$$

The photon count histograms $p[n|\alpha]$ are not directly affected by the rates if $\{R_j\} \ll \Delta t^{-1}$. Nevertheless, every measurement $n(t_i)$ provides information about the rates since Eq. (2) updates our knowledge by predicting an *a priori* distribution for the generalized probabilities $p^{\text{pri}}(\alpha, \{R_j\})$.

We take an initially flat probability distribution (no knowledge) for the rates and evaluate the probabilities on a discrete grid in the four dimensional space of states and rates for each measurement $n(t_i)$. The probability values for any rates or states alone can be calculated using the marginalization rule, e.g.,

$$p^{\text{post}}[\alpha | n(t_i)] = \sum_{\{R_j\}} p^{\text{post}}[\alpha, \{R_j\} | n(t_i)]. \tag{4}$$

An example of the time evolution of a free running, weakly repumped system is given in Fig. 2(b) for the state probabilities p_α^{post} and in (c) for the distribution of rates R_{10} and R_{21} where, with increasing data accumulation (information gain), a narrow peak emerges. The transition rates and errors are extracted as the expectation values and the root mean square values of the probability distribution. We stop data acquisition when the uncertainty of the transition rates is approximately 10% yielding rates $R_{10} = (50 \pm 6)\text{s}^{-1}$, $R_{21} = (35 \pm 4)\text{s}^{-1}$, and $R_r = (59 \pm 5)\text{s}^{-1}$, where 5.1 s of data acquisition (~ 250 quantum jumps) were used. Compared to Ref. [13] a significantly lower number of quantum jumps is needed to achieve the same accuracy with this method.

Theoretically, the Bayesian data analysis is independent of the choice of bin time for $\Delta t \leqslant R_i^{-1}$ for shot noise limited signals. Experimentally, the analysis yields constant rates in the range of $\Delta t = 0.3$ ms ... 10 ms. Below $\Delta t = 0.3$ ms we observe an increase of the extracted transition rates due to a super-Poissonian broadening of the photon count histograms $p[n|\alpha]$ [13]. We attribute this broadening to atom-cavity coupling fluctuations induced by atomic motion. They cause correlations not accounted for by the Bayesian state estimation, which leads to noise affecting the rate estimation. They are more relevant at short bin times where the photon number distributions $p[n|\alpha]$ are not well separated. We have thus chosen a bin time of $\Delta t = 1$ ms which maintains high time resolution while providing acceptable separation of the photon count histograms. Before closing the feedback loop we measure the photon count histograms and determine the rates R_{21},R_{10} according to Eq. (3).

In order to steer the system towards the target state $\hat{\rho}_{\alpha=1}$ we continuously monitor the cavity transmission and use Eqs. (1) and (2) for real-time state estimation of the state probabilities. The algorithm controlling the application of short, intense pulses of repumping and depumping laser light minimizes the Kolmogorov distance [17] $D[\mathbf{p}_{\text{target}}, \mathbf{p}(t_i)] = \frac{1}{2}\sum_\alpha |\mathbf{p}_\alpha^{\text{target}} - \mathbf{p}_\alpha(t_i)|$. This distance quantitatively measures the difference of the estimated time-dependent probabilities from the target state and is equal to maximizing $p_1(t_i)$ in case of $\mathbf{p}_\alpha^{\text{target}} = (0, 1, 0)^{\text{T}}$.

The short laser pulses drive state changes with transition probabilities $T_{\text{r,d}}$ during a single pulse of length δt. This knowledge is included in our algorithm by multiplying $\mathbf{p}^{\text{post}}(t_i)$ with a matrix

$$\mathbf{M}_r = \begin{pmatrix} (1 - T_r)^2 & 0 & 0 \\ 2T_r(1 - T_r) & 1 - T_r & 0 \\ T_r^2 & T_r & 1 \end{pmatrix}, \tag{5}$$

for a repumping laser pulse and accordingly $\mathbf{M}_d$ for a depumping pulse. The optimal transition probabilities can then be calculated by minimizing the distance $D[\mathbf{p}_{\text{target}}, \mathbf{M}_i \mathbf{p}^{\text{post}}(t_i)]$ with respect to T_i. Here, the optimal T_i depend on $\mathbf{p}(t_i)$ and lie within a range of [0.25, 0.5] per pulse. However, simulations show that the mean occupation of the target state does not change significantly if the algorithm is simplified as follows: We use a fixed value of $T_r(T_d)$ and apply a repumping (depumping) laser pulse if $p_0(t_i) > p_1(t_i), p_2(t_i)$ $[p_2(t_i) > p_0(t_i), p_1(t_i)]$, respectively. Since this feedback method is less demanding to be technically implemented, we have experimentally set $T_{\text{r,d}}$ to values that maximize the estimated probability of the target state by fixing the length of the pulses to $\delta t \approx 1.5$ μs and optimizing its intensity. The computation of the closed feedback loop algorithm takes a time of about 6 μs on our digital signal processor (TMS6713 by Texas Instruments) and can thus be neglected with respect to the update frequency of 1 ms^{-1}.

A typical measurement of the probe transmission with feedback is plotted in Fig. 3. The vertical lines in the

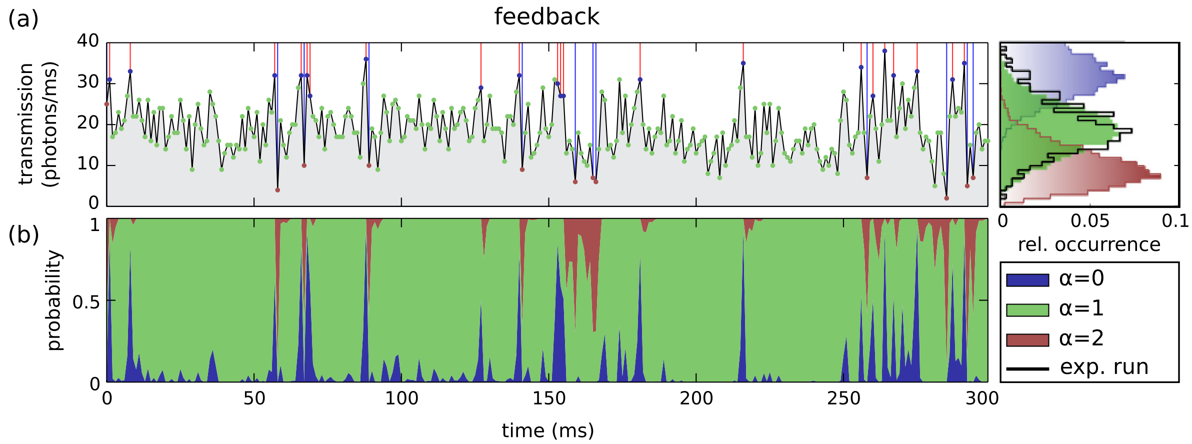

FIG. 3 (color online). (a) Detected number of transmitted photons $n(t_i)$ through the cavity while feedback onto the two-atom state $\hat{\rho}_{\alpha=1}$ is applied. The vertical lines indicate repumping and depumping feedback pulses, respectively. Note that the photon count histogram of $n(t_i)$ (black) resembles the histogram for exactly one coupled atom to a high degree as shown in the right figure. (b) Estimated Bayesian state probabilities $p_\alpha^{\text{post}}(t_i)$ calculated in real time.

background of the transmission data indicate a repumping and depumping laser pulse. The random telegraph pattern of the quantum jumps is strongly suppressed and the state probabilities are dominated by p_1. Furthermore, the photon-count histogram of the experimental feedback trace (black) is almost identical with the photon count histogram of a single coupled atom ($\alpha = 1$, green), confirming the reliability of our state estimation and feedback scheme. In principle an out-of-loop measurement of the atomic states could be performed via a push-out technique [18].

The mean probability of the target state $\hat{\rho}_{\alpha=1}$ over many experiments is $\langle p_1^{\text{post}}(t_i)\rangle = 84\%$, see Fig. 4(a). This is in excellent agreement with a Monte Carlo simulation of the feedback based on the measured rates R_{21}, R_{10} and the measured photon count histograms $p[n|\alpha]$. The scheme is also capable of stabilizing the states $\hat{\rho}_{\alpha=0,2}$, but these states are trivially accessible by optical pumping.

The time constant for the atom-cavity system to stay in $\hat{\rho}_{\alpha=1}$ is determined to be $\tau = (19 \pm 2)\text{ms} \approx 1/R_{10}$, in full agreement with the prediction by the rate equations: The mean time in state $\alpha = 1$ is ultimately limited by inelastic scattering of the probe laser with rate R_{10} yielding a probability of $1 - R_{10}\Delta t$ to stay in this state during a time bin Δt. The effectivity of the feedback loop is characterized by the time constant until the target state is reached which is experimentally given by 1.12 ms and thus, near the theoretical optimum of a single time bin. The slightly larger mean probability of the lowest state $\hat{\rho}_{\alpha=0}$ compared to $\hat{\rho}_{\alpha=2}$, visible in Fig. 4(a). is caused by the depumping due to the probe laser.

Without feedback the highest passively achievable mean probability of the target state $\hat{\rho}_{\alpha=1}$ is 50% for saturating repumping and depumping lasers. In this limit, the pumping lasers dominate the system dynamics and cause very high transition rates. In a more appropriate case of a weak continuous repumping laser ($R_\text{r} = 59\text{s}^{-1}$) we have experimentally determined the mean probability $\langle p_1^{\text{post}}(t_i)\rangle = 33\%$, see Fig. 4(c). The solution of Eq. (2) for traces of 300 ms length under the same initial condition of $\mathbf{p}(t_0) = (0, 0, 1)^\text{T}$ depending on the repumping rate R_r yields the expected mean probability as a function of R_r, see Fig. 4(d). Even at an optimal repumping rate, the mean target state probability never exceeds 37%, see Fig. 4(b).

In order to increase the mean target state probability we have to minimize the error probability $R_{10}\Delta t$ of leaving the target state within a time bin while maintaining the

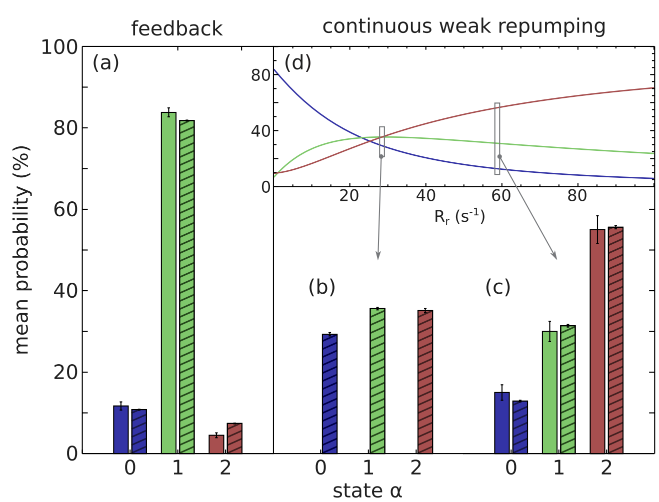

FIG. 4 (color online). Comparison of mean probabilities for the case of feedback (a) and continuous weak repumping experiments for measured (c) and optimal repumping rate (b). The shaded bars indicate simulated results. (d) Analytical solution of the mean probabilities for different repumping rates R_r.

separation of the photon count histograms as discussed above. The error minimization could be realized by a reduction of the optimal bin time Δt or the transition rate R_{10} although these variables are not independent in general: The first depends on our 4.4% detection efficiency of the transmitted light [13]. An enhancement by a factor of two of the detection efficiency would lead to a separation of the photon count histograms allowing us to reduce the bin time and thus the error probability $1 - \langle p_1^{\mathrm{post}}(t_i)\rangle$ by the same factor. Also improving localization of the atoms inside the cavity by means of an additional dipole trap would allow us to reduce the width of the photon count histograms to Poissonian shape and increase $\langle p_1^{\mathrm{post}}(t_i)\rangle$ to 86%. In cavities with a very high single atom cooperativity C a further enhancement of the cavity-atom detuning would result in a reduction of $R_{10} \propto 1/C$ which would decrease the error probability linearly.

The mixed state $\hat{\rho}_{\alpha=1}$ that has been stabilized in our experiment can be viewed as a statistical mixture of the two Bell states $|\Psi^{\pm}\rangle = (|\uparrow\downarrow\rangle \pm |\downarrow\uparrow\rangle)/\sqrt{2}$, which are indistinguishable by the projective transmission measurement employed here. In order to extend the feedback scheme to entangled states, one could use the fact that the state $|\Psi^{-}\rangle$ is the only eigenstate of a successive application of a common $\pi/2$ single qubit rotation of both atoms and the transmission measurement with a transmission level of $\alpha = 1$. Any contribution from $|\Psi^{+}\rangle$ will be projected onto the states $\hat{\rho}_{\alpha=0(2)}$ after a sufficient number of repetitions. Thus, a future quantum feedback algorithm might utilize this measurement scheme to detect and purify the entangled state $|\Psi^{-}\rangle$ and to restore it in case of $\hat{\rho}_{\alpha=0(2)}$: For this one could create $|\Psi^{+}\rangle$ according to a probabilistic scheme proposed by Sørensen and Mølmer [8] and convert $|\Psi^{+}\rangle$ to $|\Psi^{-}\rangle$ with a differential phase shift between the two atoms, e.g., by a magnetic field gradient. This stabilization scheme would require a total photon scattering of less than a single photon per atom state detection [19].

We acknowledge financial support by the EC through AQUTE and CCQED and by the BMBF through QuOReP. R. R. acknowledges support from the Studienstiftung des deutschen Volkes and R. R. and M. M. D. acknowledge support from the Bonn-Cologne Graduate School of Physics and Astronomy.

*brakhane@iap.uni-bonn.de

[1] L.-M. Duan, M. D. Lukin, J. I. Cirac, and P. Zoller, Nature (London) **414**, 413 (2001).
[2] M. Saffman, T. G. Walker, and K. Mølmer, Rev. Mod. Phys. **82**, 2313 (2010).
[3] R. Blatt and D. Wineland, Nature (London) **453**, 1008 (2008).
[4] R. Blatt and C. F. Roos, Nature Phys. **8**, 277 (2012).
[5] I. Bloch, J. Dalibard, and S. Nascimbène, Nature Phys. **8**, 267 (2012).
[6] A. A. Houck, H. E. Türeci, and J. Koch, Nature Phys. **8**, 292 (2012).
[7] L. You, X. X. Yi, and X. H. Su, Phys. Rev. A **67**, 032308 (2003).
[8] A. S. Sørensen and K. Mølmer, Phys. Rev. Lett. **91**, 097905 (2003).
[9] C. Sayrin, I. Dotsenko, X. Zhou, B. Peaudecerf, T. Rybarczyk, S. Gleyzes, P. Rouchon, M. Mirrahimi, H. Amini, M. Brune *et al.*, Nature (London) **477**, 73 (2011).
[10] V. I. Balykin and V. S. Letokhov, Phys. Rev. A **64**, 063410 (2001).
[11] M. Koch, C. Sames, A. Kubanek, M. Apel, M. Balbach, A. Ourjoumtsev, P. W. H. Pinkse, and G. Rempe, Phys. Rev. Lett. **105**, 173003 (2010).
[12] A. Kubanek, M. Koch, C. Sames, A. Ourjoumtsev, T. Wilk, P. W. H. Pinkse, and G. Rempe, Appl. Phys. B **102**, 433 (2011).
[13] S. Reick, K. Mølmer, W. Alt, M. Eckstein, T. Kampschulte, L. Kong, R. Reimann, A. Thobe, A. Widera, and D. Meschede, J. Opt. Soc. Am. B **27**, A152 (2010).
[14] D. S. Sivia and J. Skilling, *Data Analysis: A Bayesian Tutorial* (Oxford University Press, Oxford, 2006), 2nd ed..
[15] M. Khudaverdyan, W. Alt, I. Dotsenko, T. Kampschulte, K. Lenhard, A. Rauschenbeutel, S. Reick, K. Schörner, A. Widera, and D. Meschede, New J. Phys. **10**, 073023 (2008).
[16] M. Khudaverdyan, W. Alt, T. Kampschulte, S. Reick, A. Thobe, A. Widera, and D. Meschede, Phys. Rev. Lett. **103**, 123006 (2009).
[17] I. L. C. Michael and A. Nielsen, *Quantum Computation and Quantum Information* (Cambridge University Press, Cambridge, 2010), 10th ed.
[18] D. Schrader, I. Dotsenko, M. Khudaverdyan, Y. Miroshnychenko, A. Rauschenbeutel, and D. Meschede, Phys. Rev. Lett. **93**, 150501 (2004).
[19] J. Volz, R. Gehr, G. Dubois, J. Esteve, and J. Reichel, Nature (London) **475**, 210 (2011).